AIAA JOURNAL
Vol. 43, No. 7, July 2005

Damage Tolerance and Fail Safety of Welded Aircraft Wing Panels

Xiang Zhang*
Cranfield University, Bedford, England MK43 0AL, United Kingdom
and
Yazhi Li†
Northwestern Polytechnical University, 710072 Xi'an, People's Republic of China

An investigation is presented on fatigue crack growth behavior and fail safety of integral stringer panels typified by welded aircraft fabrications. The stringer panel is made of aluminum alloy 2024-T351 and fabricated by the variable-polarity plasma-arc welding process. The sample simulates a part of the lower-wing skin structures. Based on the linear elastic fracture mechanics, numerical simulations are performed for two configurations, two-stringer and nine-stringer panels, and three damage scenarios, in which welding-induced longitudinal residual stresses are taken into account. A typical load spectrum for large transport aircraft is employed for the analysis. For the two-stringer panel life predictions have a reasonably good correlation with the test results. Based on this validation, large-scale nine-stringer panels with three manufacture options, that is, riveted, integrally machined, and welded integral, are simulated for a skin crack under a broken central stringer propagating to two-bay length. Useful comparisons are made among the three variants. Finally, remedies to improve damage tolerance and fail safety of integral stringer panels are explored. The incorporation of crack retarder straps bonded to the inner surface of an integral panel has greatly improved the fail safety behavior of the component with dramatically increased crack growth live.

Nomenclature

A_{el}	=	equivalent adhesive area modeled by a spring element
A_{st}	=	stringer cross-section area
a	=	half crack length
b	=	distance between two adjacent stringers (bay width)
E_a	=	Young's modulus of the adhesive
$f_{x,i}\, f_{y,i}\, f_{z,i}$	=	spring forces
K_C	=	critical stress intensity factor under plane-stress condition
$K_{\max}$, $K_{\min}$	=	maximum, minimum stress intensity factor under applied stress cycles
K_{open}	=	crack-opening stress intensity factor
K_{residual}	=	stress intensity factor caused by welding residual stresses
t	=	thickness of skin sheet
β	=	coefficient of stress intensity factor
ΔK	=	applied stress-intensity-factor range
ΔK_{eff}	=	effective stress-intensity-factor range
σ_i	=	peeling stress in adhesive
$\sigma_{\max}$	=	maximum cyclic stress
σ_{open}	=	crack opening stress
τ_i	=	geometrical average of two transverse shear stresses in adhesive
τ_u	=	shear strength allowable of adhesive
$\tau_{x,i}\, \tau_{y,i}$	=	transverse shear stresses in adhesive

Introduction

STRINGER stiffened panels have been employed by the commercial transport aircraft manufactures for more than 50 years. In terms of traditional manufacturing process, there are two types of stiffened panels: integrally machined and mechanically fastened (also known as riveted or built up). The former results in very high scrap rate of expensive aerospace aluminum alloys, whereas the latter relies on some thousands of fasteners to assemble stiffeners to the skin sheet. Therefore, joining aircraft structures by welding technique is attractive and the subject of current intensive research by the aerospace industry and academia.[1] Adhesive bonding is another joining approach and was developed well before the initiative of welding aerospace aluminum parts.[2] It is an old technique, and not as widely used at present as it once was. The main drive of these alternative joining methods is to reduce the manufacturing costs by eliminating the expensive and time-consuming riveting operations. This paper investigates the damage tolerance and fail safety aspects of a welded stringer panel used in aircraft wing design.

Welded stringer panels are regarded as integral structures that must satisfy the necessary requirements on mechanical performance that is achieved by using the current built-up structures. One of such requirements is the damage tolerance and fail safety capability.[3–5] The damage tolerance approach assumes that there are initial cracks existing in structures caused by manufacture defects or maintenance handling and that the fatigue life of the structure is consumed with slow crack growth up to the critical crack length at which failure will occur on the application of the design limit load. Safety is ensured by inspections at which growing cracks can be detected with 90% reliability and 95% confidence. The fail-safe design philosophy states that aircraft shall be designed so that it has capability to continue in service after the failure of major components or structures. Design features, such as multiple load paths and crack stoppers in which the structure is capable of bearing design limit load after the failure of one major part, are an integral part of a fail-safe design. Although the two-bay crack criterion is not a regulatory requirement, it is often an aim for the wing and fuselage panel design.

To design damage-tolerant welded stringer panels, it is necessary to review the advantages and limitations of integrally machined and built-up stringer panels. Riveted stringers act as crack stoppers improving fail safety considerably.[3–5] However, fastener holes are stress raisers and can cause premature initiation of fatigue cracks. On the other hand, integral panels have far superior fatigue resistance to that of built-up panels, which partially compensates for the absence of the crack-stopping capabilities that are obtained with

Received 20 April 2004; revision received 8 December 2004; accepted for publication 7 January 2005.

*Senior Lecturer, Aerospace Engineering Group, School of Engineering. Member AIAA.
†Associate Professor, College of Aeronautics.

built-up construction. Recent advances in welding techniques to join aerospace aluminum materials have enabled fabricating integral structures with much reduced manufacturing cost. The friction stir welding and laser-beam welding and two plasma welding processes, metal inert gas and variable-polarity plasma arc (VPPA), have all shown excellent fatigue endurance for longitudinal weld joints in fuselage and wing stringer panels[1,5–7]; the fatigue crack initiation life of welded joints is significantly superior to that of conventionally riveted joints. Using longitudinal welded joints in surface panels also improves visual inspection capability that would be a major asset to welded integral structures. However, there are two potential problems with welded structures from the damage-tolerance viewpoint. First, welded stringer panels lack any redundant members that are important features to fail-safe design. Second, experiments have indicated a considerable increase in crack growth rates in the heat-affected zone (HAZ) as a result of welding-induced residual stresses.[7]

There have been significant research efforts directed to the fail-safe design of riveted panels,[3–5,8–12] but only a few published works on integral panels. Nesterenko investigated the residual strength of riveted and integral stringer panels made of D16 alloy (similar to 2024-T3) with the scenario of skin crack under a broken central stringer[8] and found that the difference between the two panels was insignificant for a two-bay crack length. Nesterenko[9] carried out tests on wide skin sheets and obtained R-curves to characterize the capability of material to withstand stable crack growth; for 2024-T3 alloy the critical crack length predicted by R-curves is significantly longer than that predicted by a fixed fracture toughness value caused by the tearing resistance behavior of the alloy. R-curves were then developed for the stiffened skin panels.

In terms of fatigue crack growth, the majority of work has also focused on the built-up constructions. Collins et al.[10] investigated two typical failure scenarios for cracked wing panels, primary crack in skin, and secondary crack in stringer, or vice versa. Good correlation was found between fatigue test result and prediction using an Airbus in-house analysis procedure, which incorporates parameters of stringer stiffness, sheet stiffness, and fastener flexibility. Residual strength was calculated by the R-curve technique. Hunt et al.[11] reported an Airbus wing design procedure combining crack growth and residual strength calculations with rivet and stringer static strength to ensure accurate and optimal sizing capabilities. Based on two damage-tolerance scenarios (same as those in Ref. 10), a methodology was proposed to optimize the key design parameters, that is, skin thickness and stiffener to skin area ratio, under certain constraints such as damage scenario, limit to fatigue stress ratio, and wing end loads, etc. The method was successfully applied to wing design. Less work has been published relating to integral wing panels. The early work by Poe on fatigue crack growth of bolted and integral stringer panels[12] found that the bolted stringers reduced the crack growth rate significantly, whereas the integral stringers had no significant effect. This conclusion was supported by validation fatigue tests. The stiffeners considered were unflanged (a very popular design because of their easy machining at low cost). The bay width of 50 mm might not represent the typical pitch for current large passenger aircraft wing skin panels, which should be around 75–120 mm (Ref. 13). Therefore, the problem should be revisited with a realistic pitch size and stringer section. According to Refs. 13 and 14, optimum integral stringer of compression panels should have Z-section. Recently, Nesterenko[8] compared integral and riveted panels and found that fatigue crack growth lives in both panels are practically identical when the initial damage is a skin crack beneath a broken central stringer or a skin crack between adjacent stringers provided that the skins of integral and riveted panels are fabricated of the same material, D16 alloy in this case. Examining his work we have noticed that the outer stringers for both types of panel were allowed to fail after the skin crack passed by the stringer. Therefore, the difference between the two panels in both fail-safety (two-bay crack) and damage tolerance is marginal. In reality, the riveted stringers are likely to survive after a skin crack has passed by it, especially if the stringers are made of high strength alloys, for example, the commonly used 7075-T6 alloy.[3–5]

There have been research programs devoted to crack growth behavior under the influence of welding residual stresses and microstructural changes in the HAZ, but all were performed with simple plates.[1,6,7,15,16] Although the work in Ref. 8 provides useful information on the difference between riveted and integral panels, crack growth behavior in the HAZ will be different, and the significance of this on damage-tolerance design needs to be investigated.

The main objectives of this work are to investigate fatigue crack growth behavior of welded integral stringer panels and to explore fail-safety design options for integral structures. The analysis is performed using the linear elastic fracture mechanics (LEFM) and the finite element method (FEM). Two design configurations are employed: a two-stringer panel for fatigue analysis and validation by experimental tests and a realistic nine-stringer panel for comparison with a riveted panel of the same geometry. Finally, in a novel development the influence of bonded straps to act as crack growth retarders is explored using the same analysis techniques.

Stringer Panels Studied in This Paper

Two-Stringer Panels

These panels are designed for fatigue testing. Restricted by the capacity of fatigue test machine and constraints on weld joint thickness (7 mm), it was only possible to build two-stringer panels. VPPA welding was employed to connect stringers to skin sheet. It is a welding process that produces the fusion and subsequent joining of the work-piece material by means of a highly constricted variable polarity arc.[17] In this study the stringers and skin panels were made of 2024-T351 aluminum alloy and were joined at the stringer-web near to the skin doubler as shown in Fig. 1a. The initial thickness of the weld joint was 12.5 mm; after postweld machining the finished thickness was 7 mm. To save material, the weld joints were kept as close to the skin doubler as possible. Subsequent to the optimization procedure developed in simple plates of the same material, full-length stringer panels were welded by adjustable keyhole mode operation. Distortion (bowing) after welding was less than 5 mm over a panel span of 1440 mm, and very low levels of weld defects and porosity were observed.[17] The tensile properties in aluminum alloy 2024-T351 (Ref. 7) are given here: Young's modulus, 72 GPa; 0.2% yield strength, 371 MPa; ultimate tensile strength, 477 MPa; and elongation, 18.4–21%.

To make comparisons with riveted panels used in the current large transport aircraft, I and J stringers were adopted for the tension and compression panels representing, respectively, the lower and upper surfaces of aircraft wing. Figure 1 shows the two design configurations with the longitudinal weld joints being placed at the stringer web at 12 mm from the skin-doubler, for this is the minimum operational distance required by the access of welding equipment. The stiffener to skin area ratio (A_{st}/bt) is defined as the ratio of the stiffener cross-section area to the product of the bay width and skin thickness; it is 1.03 for the tension panel (Fig. 1b) and 0.87 for the compression panel (Fig. 1c). The skin doublers are considered necessary to ease the welding residual stresses and to reduce the stress intensity factor of a skin crack. In this study, the doubler's cross-section area is counted as the stiffener area.

Welding-induced residual stresses in the two-stringer panels are measured by a neutron diffraction technique.[16] The longitudinal residual stress field is schematically illustrated in Fig. 2; the maximum tensile stress is about 150 MPa, and the maximum compressive stress is about 75 MPa. This paper focuses on the tension panel for which damage tolerance is most critical to aircraft design. The upper wing surface is designed predominantly by static criteria and to a lesser extent by fatigue.[11] Finite element (FE) static load analysis was performed for the compression panel that indicates no noticeable change in the critical buckling load as a result of the existence of welding residual stresses.

Nine-Stringer Tension Panel

This is a generic form of multiple-stringer stiffened panel designed for numerical studies. Two panels are designed, one integrally machined and the other riveted having the same geometry as shown

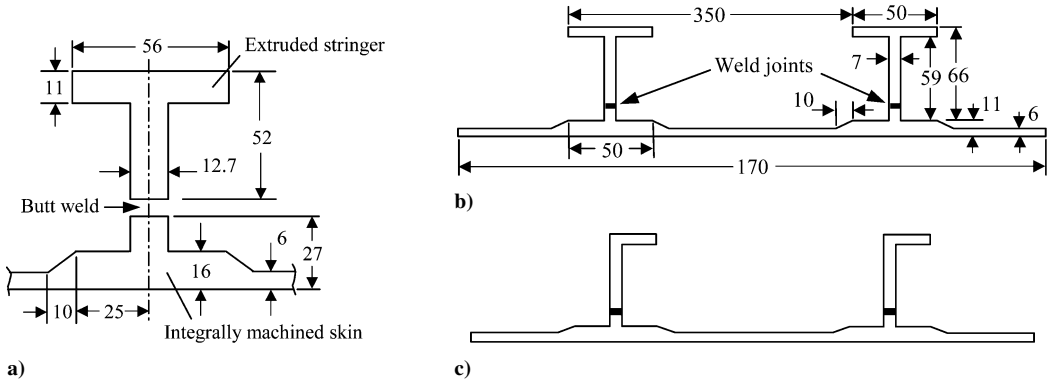

Fig. 1 Two-stringer panels fabricated by VPPA welding process: a) dimensions before welding, b) tension panel representing wing lower cover (A_{st}/bt = 1.03), and c) compression panel representing wing upper cover (A_{st}/bt = 0.87) (all dimensions in millimeters).

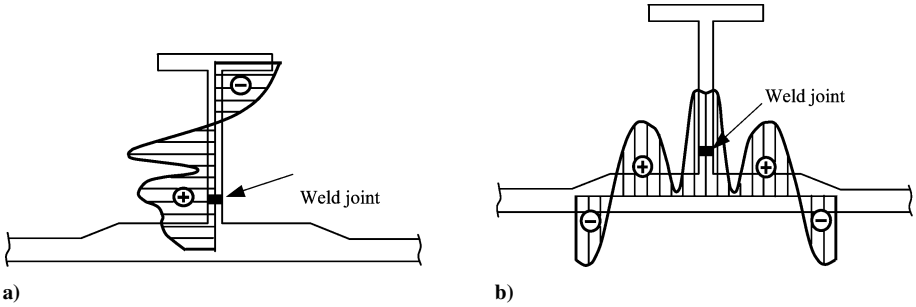

Fig. 2 Schematic of residual stress distributions in welded stringer panels (longitudinal direction): a) residual stress field along the stringer web and b) residual stress distribution along the skin-doubler.

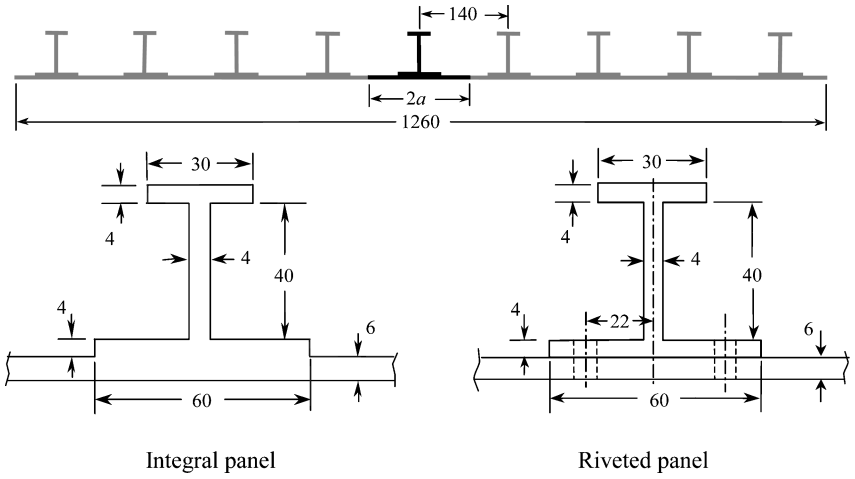

Fig. 3 Nine-stringer panels for generic analysis (A_{st}/bt = 0.62). This geometry was used for three cases: riveted, integrally machined, and welded integral panels, for comparison in damage tolerance and fail-safety performance.

in Fig. 3. These wider panels allow us to study the scenarios of skin crack growth either under a broken stringer or between two adjacent stringers and make comparisons among integrally machined, welded integral and riveted panels. The material used for fabricating the skin sheets and stringers is aluminum alloy 2024-T351. The stiffener to skin area ratio is 0.62 for both configurations.

Damage-Tolerance Analysis

Failure Scenarios

For this study, we have chosen a two-bay crack length as an arbitrary critical crack length for residual strength check. It is not a universal failure criterion for the design of stiffened wing panels, and it is often desirable but still not a regulatory requirement. Three failure scenarios have been selected for the damage-tolerance analysis.

The first failure scenario is crack propagation from a flaw at the weld joint (Fig. 4a), where weld defects and porosity can exist. Once a crack initiates under cyclic loads, it will propagate faster under the influence of tensile residual stresses in the HAZ. The stringer will eventually fail, and the crack propagates into the skin resulting in the second failure scenario: a two-bay skin crack with a broken central stringer (Fig. 4b). The same failure mode also exists for the riveted panels. According to Swift,[5] fatigue crack can initiate in stiffeners in the wing lower surface at fuel transfer slots or at rib connection fittings. Because this damage might not be immediately detected, continued cyclic loading will cause extremely high load transfer at the first fastener causing stringer failure. Then the stringer load will be transferred to the skin creating a skin crack, which will eventually propagate into two adjacent skin bays. This

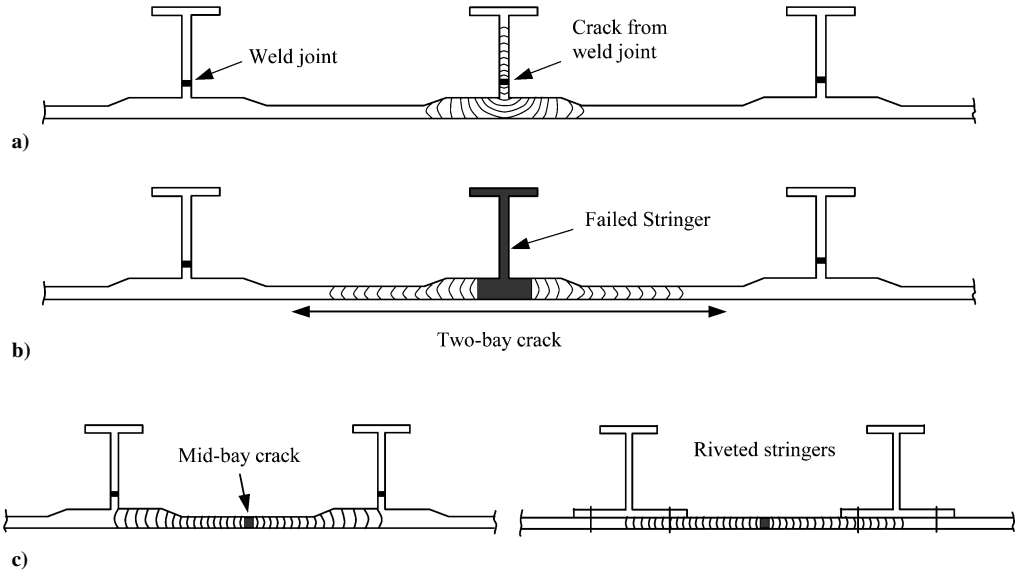

Fig. 4 Failure scenarios: a) stringer failure due to initial flaws in weld join, b) skin crack growth under a broken central stringer, and c) midbay skin cracks in integrally machined and riveted panels.

failure mode also represents a discrete source damage caused by fragments from a failed engine, which spans from one bay to the other bay and severs one stringer. The goal of this study is to provide the two-bay damage capability at the design limit load. The third damage scenario is a midbay skin crack growing toward two adjacent stringers (Fig. 4c). The riveted stringers are effective crack retarders caused by crack bridging mechanism. In contrast, integral stringers are not so effective because of the lack of redundancy structural members, which is characteristic of attached (either mechanically or bonded) stiffeners. On the other hand, an integral panel should have slower crack growth rate around the stringer and skin junction as a result of the complete rigid connection.

Analysis Methods

Stress intensity factor (SIF) is calculated by the finite element method employing the MSC NASTRAN package. The SIF range ΔK is then modified by the effects of cyclic plasticity (crack closure) and welding residual stresses through the argument of the effective stress-intensity-factor range ΔK_{eff}. One way of doing this is to perform elastoplastic FE analysis of crack growth under cyclic loads calculating crack opening stress levels and ΔK_{eff}:

$$\Delta K_{\text{eff}} = K_{\max} - K_{\text{open}} \tag{1}$$

where

$$K_{\max} = \beta\sigma_{\max}\sqrt{\pi a}, \qquad K_{\text{open}} = \beta\sigma_{\text{open}}\sqrt{\pi a} \tag{2}$$

Parameters $K_{\max}$, K_{open} and σ_{open} are determined by FE analysis under the combined residual and applied stress field.

In this work, σ_{open} is assumed to be a function of the R-ratio R and the welding-induced residual stress but not related to the structural geometry; therefore, it is possible that FE analyses for different R-ratios and welding parameters are performed on simple welded plates, and the calculated crack opening stresses (normalized by maximum cyclic stress) are applied to structures (stringer panels in this case). For a given structure, once the β (structural geometry) and σ_{open} (cyclic plasticity) are found, fatigue life prediction is carried out for a given load spectrum. This method is applied for constant amplitude loading analysis. Details of the elastoplastic analysis of welded plates and crack closure behavior are given in Ref. 18.

Residual stress caused by welding has three stress components, that is, longitudinal and transverse to the loading direction and normal to the material's thickness direction. According to the measurement in Ref. 16, the transverse and normal stress components are significantly lower than the longitudinal stress, especially in the tensile field. Our FE simulation of simple center crack tension plates shows that the stress intensity factor and crack growth rate are not sensitive to the presence of the transverse residual stress component in the FE model.[18] Therefore, in this study only the longitudinal residual stress component is included into the FE and crack growth models as an initial stress field.

An alternative approach is linear elastic by superposing the respective SIF's as a result of applied and welding residual stresses. According to the fundamental assumptions of LEFM, that is, similitude and small-scale yielding, superposition should work. The SIF range and stress ratio are calculated as

$$\Delta K = (K_{\max} + K_{\text{residual}}) - (K_{\min} + K_{\text{residual}}) \tag{3}$$

$$R = \frac{(K_{\min} + K_{\text{residual}})}{(K_{\max} + K_{\text{residual}})} \tag{4}$$

Distribution of residual stress field can be input directly into a crack growth prediction package called AFGROW,[19] which has build-in weight function and Gaussian integration facilities that will calculate the residual SIF and superpose it to the applied SIF. From Eqs. (3) and (4), the SIF range does not vary with residual stresses, but the stress ratio does, which will alter the crack opening stress level. AFGROW uses empirical laws (e.g., the NASGROW equation) to account for the crack closure effect. In this study this method is employed for variable amplitude loading spectra.

Fatigue Crack Growth Life

Stringer Web Failure

For the two-stringer tension panel, fatigue tests were performed with an initial crack of 6 mm in one stringer at the center of the weld joint. This simulates the first failure scenario as shown in Fig. 4a. In the fatigue test, the crack was found to propagate almost simultaneously toward the stringer upper flange and the skin doubler. This scenario was simulated by moving the two crack tips in both directions simultaneously. The virtual crack closure technique was employed within the framework of FEM to calculate the crack-tip strain energy release rate that was then converted to the SIF. The relationship of dimensionless SIF β vs crack length and measured longitudinal residual stresses was then inputted into the AFGROW code[19] for crack growth life prediction. Figure 5 shows the prediction results for the crack tip growing toward the stringer upper flange under a constant amplitude load (Fig. 5a) and a typical service load spectrum (Fig. 5b). The Wheeler overload retardation model is used in this study. Both panels failed by the net-section-yield criterion.

The stringer web is 59 mm long. The critical half crack length is 40 mm from the weld joint toward the upper flange root. This is consistent with the measured critical crack length. For both loading cases, final crack growth lives obtained from the panel test could be accurately predicted, but the form of the crack length vs cycles curve is quite different from the test result (Fig. 5). Redistribution of residual stresses caused by crack growth was observed in test but was not incorporated in the crack growth analysis, and the differences in predicted and experimental crack growth rates might be related to this. This problem is currently under study.

For the same geometry, the predicted crack growth life for an integrally machined stringer is significantly longer than that of welded stringer, about twice longer under the same constant amplitude load and four times longer under the variable amplitude loading. This comparison indicates that if a crack initiates at the weld joint then the tensile residual stress field in the fusion and heat affect zones will accelerate the crack growth rate significantly until the crack tip has grown well out of the HAZ.

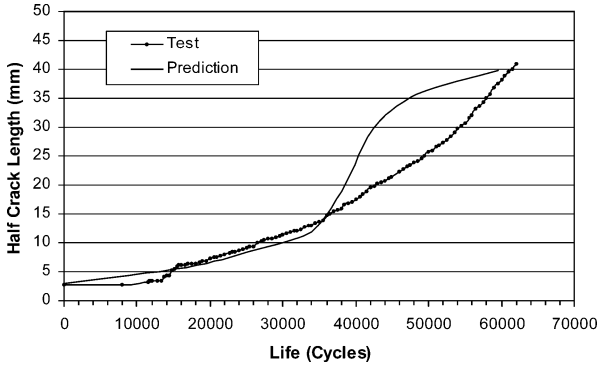

a)

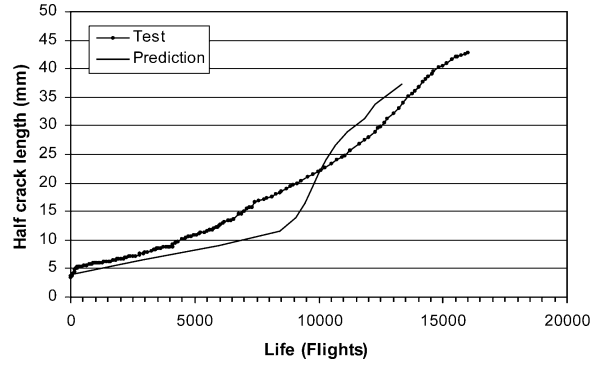

b)

Fig. 5 Fatigue crack growth life in stringer web of the two-stringer tension panel; prediction vs test: a) constant-amplitude loading (σ_{max} = 88 MPa, R = 0.1); and b) aircraft service load spectrum (σ_{max} = 138 MPa).

Skin Crack Growth Under a Broken Stringer

This analysis employs the nine-stringer panel aiming at making comparisons with a riveted panel of the same geometry. Figure 3 shows the two configurations, riveted and integrally machined; the latter can be modified to a welded integral panel by adding welding residual stresses in the analysis model. Because of the geometric symmetry, only a quarter panel is modeled as shown in Fig. 6. An assumption is made here based on the work in Ref. [12], that is, when a skin crack passes an integral stringer the crack will turn 90 deg and propagate along the stringer at the same growth rate as the skin crack (see insert of Fig. 6). This assumption can provide a conservative prediction for crack growth life. In reality, the crack growth rate along the length of the stringer might be slower than the passing skin crack; this will depend on the panel deflection, skin crack length, and the stiffener to skin area ratio. Even when the stringer crack growth slows down or is temporarily arrested, integrally machined stringers cannot act as crack growth retarders; hence, the structure is not fail safe. It is also assumed that the riveted stringers will be intact when a skin crack passes by; hence, the stringer will take considerable amount of loads from the cracked skin reducing the crack tip SIF significantly. These assumptions are realistic,[12] but one must ensure that the stress in the outer stringer does not exceed the yield strength of the stringer material.[3–5]

Figure 7 shows the variations of the dimensionless SIF β with crack length for the integral and riveted panels (FEM), and the theoretical solution of an unstiffened panel of the same width. For the riveted panel the FE result presented in Fig. 7 was validated by the displacement compatibility approach[3,5] with a few modifications made in this paper on the bending effect of the broken stringers, the finite-width correction, and approximations in dealing with the double-line riveted stringers[20]; the numerical solution of SIF agrees very well with the analytical solution. Figure 7 shows that for the unstiffened panel β increases with the growing crack length, as one would expect. For both forms of stringer panel, initially the β values are much higher than that of unstiffened panel because of the broken stringer transferring stress back to the skin. β values decrease when skin crack approaches the first outer stringer, and β of the integral panel is significantly lower (hence slower crack growth rate) than that of the riveted panel as a result of the complete rigid connection of stringer to skin. However, β of the integral panel soon increases very rapidly after the crack has passed the first outer stringer because of the crack growth along the stringer (see insert of Fig. 6). Once the crack has grown through the stringer web section, the failure of the upper flange is modeled by a sudden fracture failure; this causes an instant increase in β as indicated in Fig. 7 because part of the stringer stress is transferred to the skin. In contrast with the integral panel, β of the riveted panel decreases as the skin crack grows

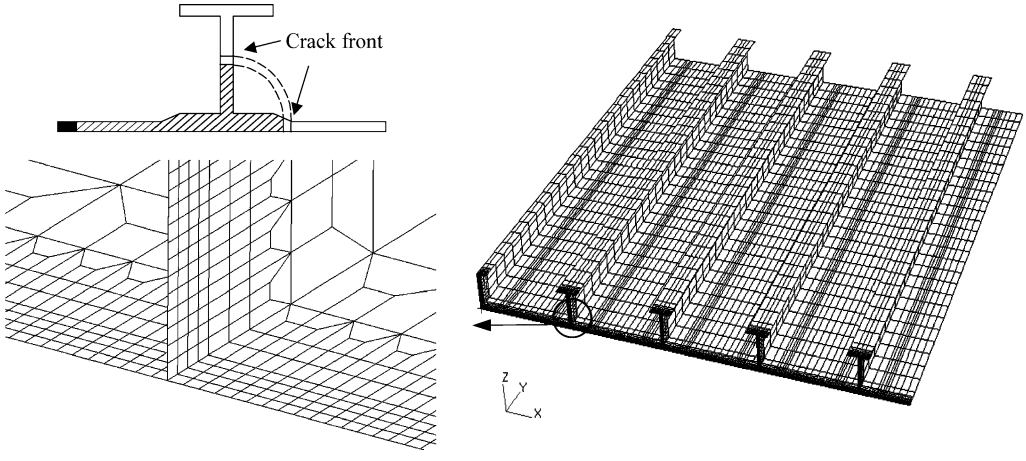

Fig. 6 FE model for $\frac{1}{4}$ of nine-stringer panel using the NASTRAN package and two-dimensional plate elements.

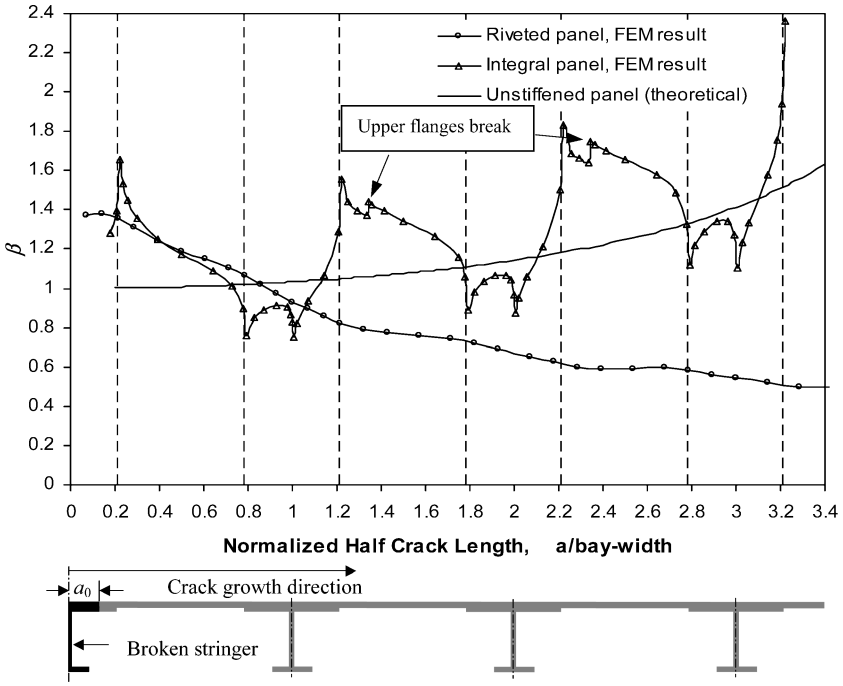

Fig. 7 Dimensionless stress intensity factor β of riveted, integrally machined and unstiffened panels.

because of the intact outer stringers that pick up more loads from the cracked skin. In our FE simulation of the riveted panel, the variation of the stringer stresses in the outer stringers is recorded as the skin crack propagates. For example, for a two-bay crack length ($a = 140$ mm) under the applied stress of 80 MPa (constant amplitude load case), the maximum von Mises stress in the first outer stringer is 211 MPa; for applied stress of 138 MPa (maximum variable amplitude stress), the maximum von Mises stress in the first outer stringer is 365 MPa, which is just under the yield stress of the material, but the maximum stress is confined in a very small region. Beyond the two-bay crack length, stringer stress increases rapidly. For example, for $a = 155$ mm under the applied stress of 138 MPa, the maximum von Mises stress in the first outer stringer is 410 MPa, which is higher than the yield strength. In this paper, stringer failure caused by yielding is not modeled, hence, the continued decrease in β even for six-bay crack length. This provides unconservative prediction of crack growth. In fact, β will increase after the first outer stringer fails. To simulate the welded integral panel, the residual stresses in the skin doublers and stringer web are inputted in the locations according to the measurement, and the corresponding residual SIF are calculated.

The initial crack length under the central broken stringer is $2a = 50$ mm. This is based on visual inspection with good detection reliability.[9] Constant-amplitude load (CAL) and variable-amplitude load representing a typical transport aircraft spectrum are applied for the computer simulation using the AFGROW code. The plane-stress fracture toughness values employed in the AFGROW (e.g., $K_C = 74\ \text{MPa}\sqrt{\text{m}}$ for 2024-T351) are far too low for this wide panel. These K_C values come from narrow panels that are net-section yield critical. For the wide nine-stringer panels we have used $K_C = 137\ \text{MPa}\sqrt{\text{m}}$, which comes from wide panel test reported in Refs. 5 and 21. In the work of Ref. 8, a higher K_C value (160–198 $\text{MPa}\sqrt{\text{m}}$) was reported for a similar alloy and same thickness.

Constant amplitude loading. Figure 8a shows the predicted crack growth lives for riveted, integrally machined, and welded panels under constant amplitude loading. First, the difference in life between the riveted and integrally machined panels is significant, 14,700 vs 7860 cycles. This is mainly because of the variations in β (Fig. 7). Initially the β of integral panel is higher than that of riveted panel until the half crack length a reaches 70 mm; hence, the crack in integral panel propagates faster. From $a = 100$ mm the β value of integral panel is significantly lower than that of riveted panel (because of the rigid connection of the integral skin doubler

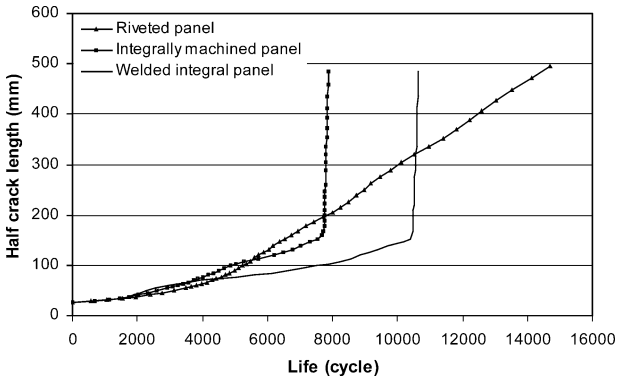

Fig. 8a Predicted crack growth lives for the nine-stringer panels: riveted, integrally machined, and welded integral. Constant-amplitude loading, $\sigma_{max} = 80$ MPa, $R = 0.1$.

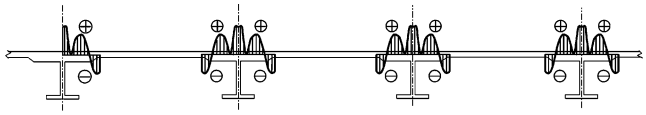

Fig. 8b Schematic of longitudinal residual stress distribution in skin-doublers. This stress field has been used for calculating the stress intensity factor caused by residual stresses.

to stringer compared to the more compliant rivet assembly), hence the much reduced crack growth rates until the crack tip is just beyond the first outer stringer ($a = 150$ mm). From then on, the riveted panel has much slower crack growth rate because of the intact outer stringers (hence much lower β values), whereas the integral panel suffers much faster crack growth rate until the final failure caused by fracture of the first outer stringer. Second, the welded integral panel has significantly longer life than that of the plain integral panel, 10,640 vs 7860 cycles. The compressive residual stresses in the skin doublers result in much reduced effective stress intensity factors for the half crack length range $a = 50$–110 mm (Fig. 8b). This phenomenon is confirmed by an experimental test for the two-stringer welded panel with an initial midbay crack of 6 mm growing toward two adjacent stringers. It is found that the crack growth rate

of the midbay crack is noticeably slower than that of a parent metal sample under the same ΔK. The residual stress fields in this case are some distance away from the skin crack and have initially negative values in the adjacent skindoublers. The influence of these compressive residual stresses was integrated into the residual SIF and added to the applied SIF forming an effective SIF that was used to calculate the crack growth rates. In summary, before the crack tip reaching the first outer stringer fatigue crack growth, lives of integrally machined and welded panels are comparable with that of the riveted panel. However, once the crack is beyond two-bay length both forms of integral panels (machined or welded) suffer much faster crack growth rate compared to the riveted variant. The riveted panel has the longest critical crack length and crack growth life and eventually fail by the net-section yield criterion, whereas both integral panels have very high SIF when the crack is just beyond two-bay length and are broken by the fracture criterion. Stringer failure caused by yielding is not considered in this paper, which will reduce the crack growth life of the riveted panel.

Variable amplitude load. Figure 9 shows the predicted crack growth lives for riveted, integrally machined, and welded panels under the same variable amplitude loading as for the two-stringer panel presented in Fig. 5b. The riveted panel has fatigue life of 7154 flights with a critical half crack length of 415 mm, while the integral panel failed at 5790 flights at half crack length of 330 mm. For the latter the practical critical half crack length is about 150 mm, which is just over two-bay length. The considerably shorter critical crack length for the integral panel is caused by the much higher stress intensity factor after the failure of two consecutive outer stringers. As shown in Fig. 7, when the crack tip has passed the second outer stringer, $a = 310$ mm, the β value reaches 1.8 resulting in very high SIF and faster crack growth rate leading to fast fracture. The simulation indicates that the riveted panel fails by the net-section yield criterion while the integral panel is broken by the fracture criterion. The welded integral panel has longest crack growth life for the same reason as discussed for the CAL load case. However, the welded panel is not regarded as a fail-safe design because the crack reaches its critical length at the first outer stringer with no attached structural members as a safe guard against any sudden catastrophic failure, whereas the riveted panel can tolerate a four-bay crack. This result was based on the assumption that crack will also propagate along an integral stringer when a skin crack passes by, while a riveted stringer will remain intact. This results in conservative estimations of the critical crack length and crack growth life in the integral panels and nonconservative estimation for the riveted panel. More accurate prediction could be achieved by calculating the crack growth rates of the skin and stringer cracks separately and taking account of the stringer failure as a result of yielding.

The crack growth pattern is complicated by the load sequence effect. The Wheeler overload retardation model is used, and the computer simulation shows a strong overload retardation effect for this type of load spectrum; without accounting for this effect, crack growth lives would be significantly underestimated. The overload effect and the use of Wheeler model are validated by the test of the two-stringer panels.

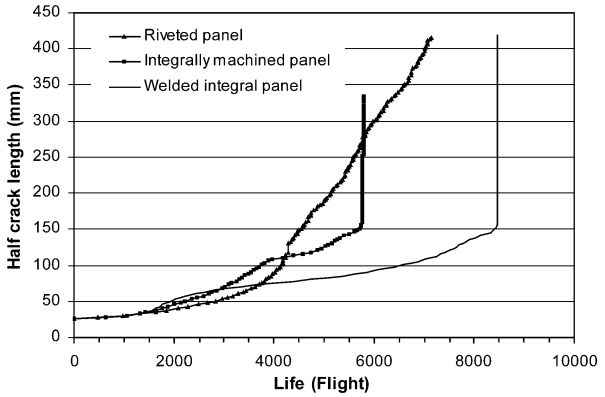

Fig. 9 Predicted crack growth lives for the nine-stringer panels (riveted, integral and welded). Variable-amplitude loading, σ_{max} = 138 MPa.

Residual Strength Analysis

For the plane-strain condition fracture toughness K_C is a material constant. However, for the plane-stress or transitional conditions K_C depends on panel's thickness as well as the width.[21,22] Therefore only the R-curve approach can accurately define the residual strength for the thickness studied here. Because of the lack of R-curve data for this very wide panel, residual strength is calculated based on the static failure criterion of linear elastic fracture mechanics, that is, $K_{max} = K_C$. The critical value used is $K_C = 137$ MPa$\sqrt{\text{m}}$ according to Ref. 5 for the same material, similar skin thickness, and stringer to skin area ratio.

For 2024-T351, it is reasonable to choose the value of 240 MPa as a typical stress level corresponding to the design limit load.[5] In reality the limit stress can be quite variable across the whole wing structure. The calculated skin fracture curves for both riveted and integral panels are shown in Fig. 10. Because of the complete rigid connection, the integrally machined panel offers higher residual strength (275 MPa) than that of riveted panel (230 MPa) at the two-bay crack length ($a/b = 1$), but before the skin crack reaches two-bay length the difference in residual strength between the two panels is not significant. However, when the skin crack is beyond the two-bay boundary, the riveted panel is performing significantly better than that of integral panel. The residual strength of riveted panel is kept just below 240 MPa for a long crack of six-bay length, while the residual strength of integral panel is dropped to a very low level. The analysis of the riveted panel did not include stringer failure caused by yielding. With the skin crack growth beyond two-bay length, the first outer stringer will break as a result of load transfer from skin to stiffeners. Therefore, both the skin fracture curve and stringer yield failure should be considered to provide accurate prediction.[3–5]

Welding residual stress was not taken into account in the residual strength analysis. It is expected that the compressive residual stresses (Fig. 8b) at the skin doublers will raise the residual strength; this is based on the skin fracture curve resulting from the β variation with the residual stresses. However, the tensile residual stresses in the welded stringers will accelerate the stringer crack growth rate. Both the positive and negative effects should be accounted in the future studies.

Fail-Safe Design Using Bonded Straps

Figures 8 and 9 indicate that both forms of integral panel have much shorter critical crack length, that is, $a_{cr} = 150$ mm (two-bay crack length), compared to $a_{cr} = 420$ mm (six-bay length) for the riveted panel. Although the residual strength at two-bay crack length is comparable for the riveted and integral panels, the latter is not regarded as fail-safe design because of the absence of redundant structural members; sudden failure will occur when the skin crack is beyond two-bay length. Therefore some forms of attached members are necessary to ensure fail safety.

In this work we have chosen adhesively bonded straps as crack growth retarders. These narrow straps are 3 mm thick and 15 mm wide and are placed 6 mm away from the doubler edge (Fig. 11a). Two materials are selected for the straps, titanium alloy Ti-6Al-4V and carbon/epoxy 6376C-HTA unidirectional (UD) laminates (24 plies). The former is highly ductile and hence will cope with larger crack opening displacement while the straps picking up loads from the cracked skin slowly and effectively; the latter is brittle but has very high tensile strength (almost double the titanium alloy strength), and so it can take much higher loads and is about 60% lighter. The bonding layer is made of FM 73 adhesive material. A typical experimental shear stress-strain relation of the adhesive gives shear strength of 37 MPa and shows large nonlinear deformation before failure by shear.[2]

In our FE model, the corresponding nodes on the overlapping strap and skin are connected by three spring elements (per connection point) to simulate the deformation of adhesive layer, two springs representing the shear deformation in two lateral directions and one

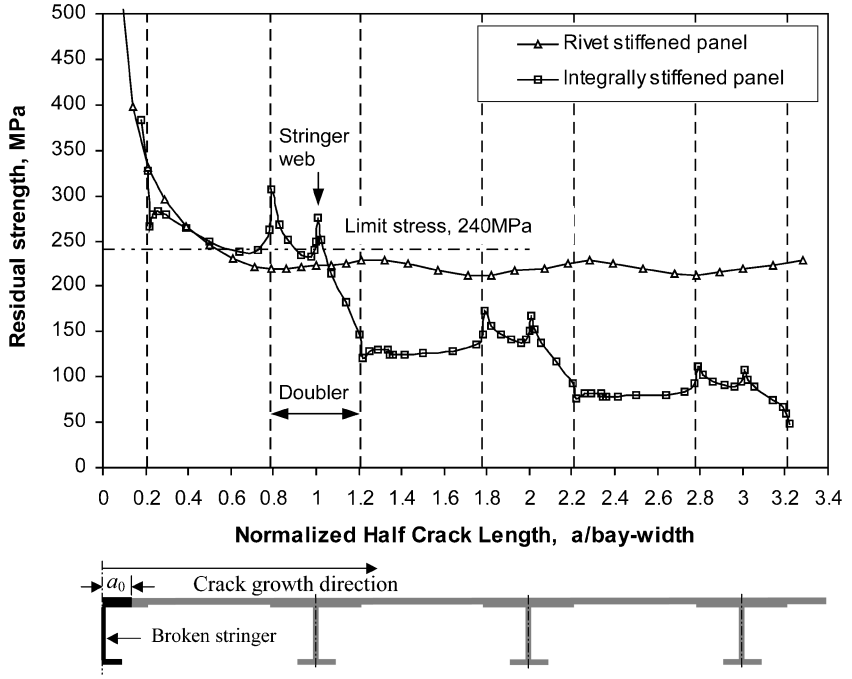

Fig. 10 Skin fracture curves for both integral and riveted panels.

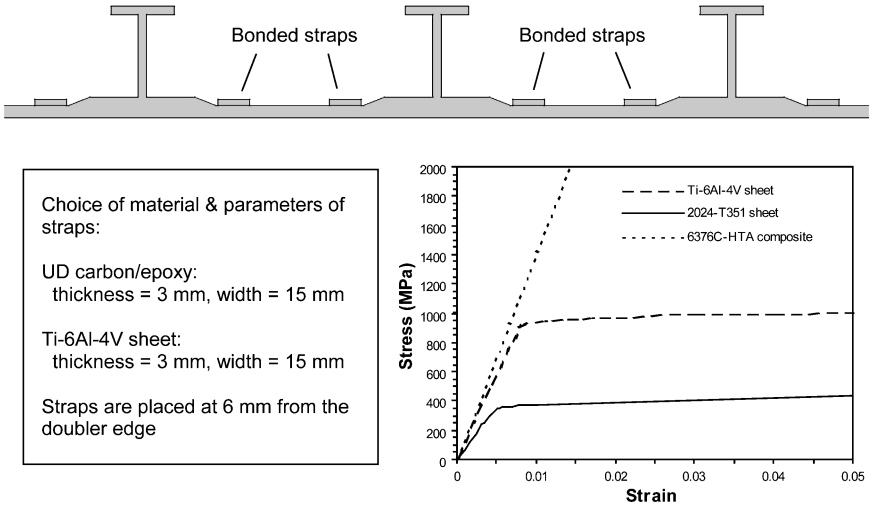

Fig. 11a Schematic of strap design considerations: geometry and material.

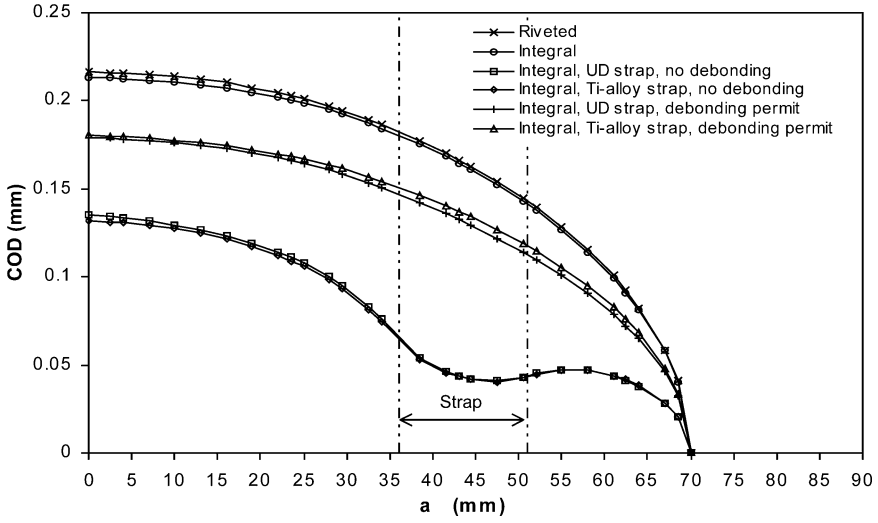

Fig. 11b Effect of bonded straps on crack-opening displacements.

mimicking the peeling action. The Young's modulus of the adhesive is $E_a = 1.92$ GPa, and the strength values are $\tau_u = 33.0$ MPa (pure shear) and $\sigma_u = 57.0$ MPa (von Mises equivalent value). The behavior of the adhesive is assumed to be elastic for simplicity in analysis. The stiffness of the spring elements is determined based on the method in Ref. 23.

At each computational iteration step, the adhesive stresses are calculated by

$$\tau_{x,i} = f_{x,i}/A_{\text{el}}, \qquad \tau_{y,i} = f_{y,i}/A_{\text{el}} \tag{5}$$

$$\tau_i = \sqrt{\tau_{x,i}^2 + \tau_{y,i}^2}, \qquad \sigma_i = f_{z,i}/A_{\text{el}} \tag{6}$$

Assuming local adhesive failure (disbond between skin and strap) occurs when

$$\sigma_e = \sqrt{\sigma_i^2 + 3\tau_i^2} \geq \sigma_u \qquad \text{for} \qquad \sigma_i > 0 \tag{7}$$

or

$$\sigma_e = \sqrt{3\tau_i} \geq \sigma_u \quad \text{for} \qquad \sigma_i \leq 0 \tag{8}$$

The debonding process is modeled in an iterative manner. When Eq. (7) or (8) is satisfied, the stiffness values of the relevant spring elements are set to zero. This is done for a small group of springs at a time to ensure computational convergence. Computed crack-opening displacement profiles are shown in Fig. 11b, demonstrating the effectiveness of the bonded straps in restricting the crack opening deformation, which is related to the effective SIF values. The effectiveness of these bonded straps depends on the amount of load that gets transferred from skin to straps with crack growth. As the crack length increases, the shear and peel stresses in the adhesive layer will also increase and eventually exceed the allowable values resulting in local disbond between the strap and panel skin. With localized disbond the straps can still carry the load but are less effective because of the lack of shear transfer capability. Figure 11b also shows the case when debonding is not modeled in the computer simulation, which is not realistic for this material, but if we use a better adhesive disbond will be delayed or avoided. Figure 12 shows the stress levels in the first bonded strap that the crack has passed and comparison with the case when disbond is not modeled; for the latter case, the tensile stress in the strap is very high reaching the ultimate tensile strength of both strap materials at two-bay crack length. For the titanium strap, the maximum stress results in gross yield of the strap. For the composite strap, the in-plane tensile stress is close to the ultimate tensile strength. The figure also shows considerable reduction in strap stress as soon as the adhesive starts to debond. The figure also indicates that the strap failure stress is never reached because of adhesive disbond; hence, the strap becomes less efficient in transferring the skin load. The composite strap is more effective than the titanium one in terms of reducing in-plane tensile loads. The variation of β vs crack length (Fig. 13) shows that using bonded straps can reduce the crack-tip stress intensity factor by about 25%. Consequently crack growth rate will be reduced even more significantly. The difference in β values is small by straps made of two different materials. Figure 14 presents the predicted crack growth life of an integrally machined panel reinforced with bonded straps made of unidirectional carbon/epoxy (geometry; see Fig. 11). In this case the AFGROW computation was terminated at the half crack length of 200 mm because the β calculation was cut short at this crack length because of the time-consuming computation, that is, elastoplastic analysis and adhesive disbond modeling. Nevertheless 200 mm is about the critical crack length when fast fracture will occur, and this example is sufficient to demonstrate the effectiveness of the bonded straps; the improved crack growth life of 20,467 flights is significant: five times of the plain integral panel. This example is a feasibility study to explore the crack bridging capability of bonded straps; hence, estimated dimensions and positions for these straps have been used. The manufacture cost of integral panels (by machining, extrusion, or welding) and adhesive bonding of discrete thin straps should be further investigated against the cost of riveted panels given that automatic riveting machines are now widely used. The material and geometry of these crack growth retarders should be optimized, and their impact on the overall load transfer and stiffness of the wing structure should also be studied.

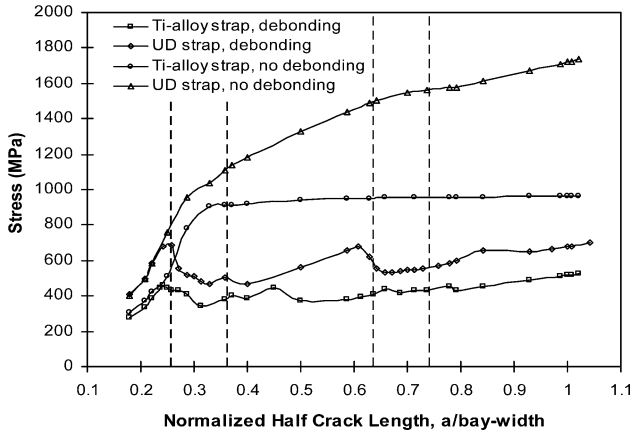

Fig. 12 Maximum in-plane stress in the first bonded strap that the crack tip has passed: von Mises stress for the titanium strap; fiber direction tensile stress for the composite strap.

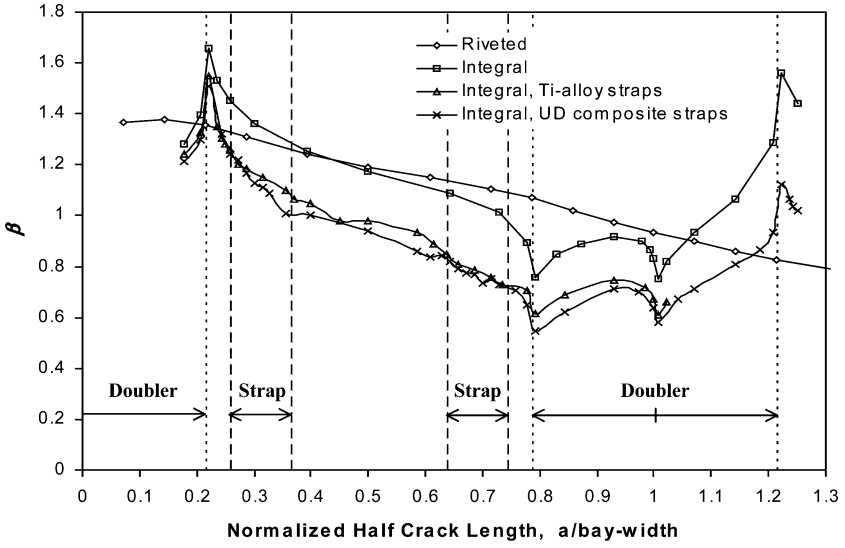

Fig. 13 Effect of bonded straps on the stress intensity factor of a two-bay crack.

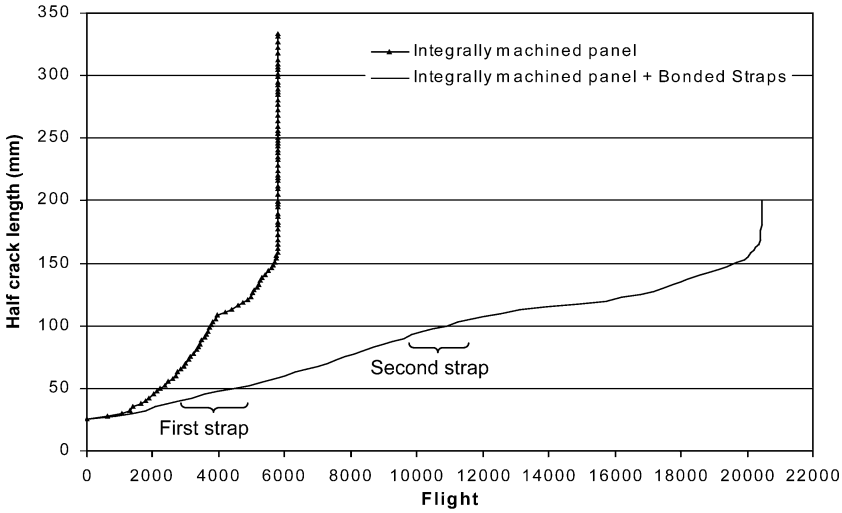

Fig. 14 Predicted crack growth lives for integrally machined panels with and without crack retarder straps; aircraft service load spectrum (σ_{max} = 138 MPa).

Conclusions

This paper has investigated the damage-tolerance and fail-safety issues of welded stringer panels used in aircraft wing design. The effect of welding residual stress on crack growth life has been taken into account in the fracture mechanics and finite element analyses. Comparison of the fatigue crack growth behavior has been made with riveted and integrally machined panels of the same geometry. The study is carried out by numerical simulation of a welded two-stringer panel and a wide nine-stringer panel; analysis of the former is validated by experimental test. The following conclusions are drawn:

For cracks initiated at the weld joint, tensile residual stresses in the fusion and heat-affected zones will accelerate the crack growth rate significantly resulting in shorter crack growth life than that of integrally machined stringer panel. For the two-stringer panel under a typical transport aircraft load spectrum, it takes about 16,000 flights for one stringer to fail due to a 6-mm initial crack at the weld joint.

Simulation of the relative performance of riveted, integrally machined, and welded nine-stringer panels indicates that 1) integral stringers (by either welding or machining) are more effective than riveted stringers in reducing the stress intensity factors at the stringer-skin connection area as a result of the former being much more rigid than the latter, consequently when a skin crack is approaching the first outer stringer crack growth rate becomes slower in the integral panels compared to the riveted panel; 2) welded integral panel has the longest fatigue crack growth life, but the worst fail safety behavior with unstable crack after the failure of two outer stringers; and 3) the much reduced crack growth rate in welded panel is also caused by the influence of welding-induced compressive residual stresses at the adjacent skin doublers. Therefore, if a crack initiates outside the HAZ and propagates between two welded stringers, then the crack growth rate is reduced.

Adhesively bonded straps are necessary and effective in increasing the residual strength and crack growth life of integrally machined and welded integral panels. In this paper a titanium alloy and a fiber-reinforced plastic are selected for making these straps representing a wide range of material behavior; numerical simulation suggests that straps made of unidirectional carbon/epoxy composite are more effective in transferring loads from a cracked skin panel.

Acknowledgments

The authors are grateful to the Engineering and Physical Sciences Research Council (GR/N14057), QinetiQ, and Airbus UK for providing financial assistance. Y. Li acknowledges the funding from the Chinese government through a visiting scholarship. In addition, they thank A. Theos for assistance in panel design, J. Lin for providing validation test, and G. Allegri and S. Mielow for performing part of the finite element analysis.

References

[1]Bussu, G., and Irving, P. E., "The Role of Residual Stress and Heat Affected Zone Properties on Fatigue Crack Propagation in Friction Stir Welded 2024 T351 Aluminum Joints," *International Journal of Fatigue*, Vol. 25, No. 1, 2003, pp. 77–88.

[2]Swift, T., "Important Considerations in Commercial Aircraft Damage Tolerance," *International Journal of Vehicle Design*, Vol. 7, Nos. 3/4, 1986, pp. 264–287.

[3]Swift, T., "Application of Damage Tolerance Technology to Type Certification," Society of Automotive Engineers, Paper Series 811065, Oct. 1981.

[4]Swift, T., "Development of the Fail-Safe Design Features of the DC-10," *Damage Tolerance in Aircraft Structures*, ASTM Special Technical Publ. 486, American Society for Testing and Materials, Philadelphia, 1971, pp. 164–214.

[5]Swift, T., "Fail-Safe Design Requirements and Features, Regulatory Requirements," AIAA Paper 2003-2783, July 2003.

[6]Lefebre, F., and Sinclair, I., "Micromechanical Assessment of Fatigue in a MIG and VPPA Welded Aluminum Airframe Alloy," *Fatigue 2002—Proceedings of the 8th International Fatigue Congress*, Vol. 1, edited by A. F. Bloom, Engineering Materials Advisory Services, Ltd., Cradley Heath, England, U.K., 2002, pp. 429–436.

[7]Lin, J., Ganguly, S., Edwards, L., and Irving, P. E., "Effects of Residual Stresses and HAZ on Fatigue Crack Growth in MIG Welded 2024 and 7150 Aluminum," *Proceedings of Fatigue 2003—Fatigue and Durability Assessment of Materials, Components and Structures*, Engineering Integrity Society, Sheffield, England, U.K., 2003, pp. 65–72.

[8]Nesterenko, G. I., "Comparison of Damage Tolerance of Integrally Stiffened and Riveted Structures," International Council of the Aeronautical Sciences, Paper 444.1, Aug. 2000.

[9]Nesterenko, B. G., "Analytical-Experimental Study of Damage Tolerance of Aircraft Structures," International Council of the Aeronautical Sciences, Paper 333.1, Aug. 2002.

[10]Collins, R., Dean, M. S., Williams, A. D., Bishop, M. A., van Griensven, B. F., and Alexander, A. M., "Fatigue and Damage Tolerance Tests in Support of the Certification of Airbus A330/A340 Metallic Wing Structure," *Proceedings of the 19th Symposium of the International Committee on Aeronautical Fatigue*, Vol. 2, edited by R. Cook and P. Poole, Engineering Materials Advisory Services, Ltd., Cradley Heath, England, U.K., 1997, pp. 955–966.

[11]Hunt, E., Williams, A. D., and Jones, M., "Fatigue and Damage Tolerance Design of Large Airbus Wing Structures," *Proceedings of the 20th Symposium of the International Committee on Aeronautical Fatigue*, Vol. 1, edited by J. L. Rudd and R. M. Bader, International Committee on Aeronautical Fatigue, 1999, pp. 111–124.

[12]Poe, C. C., Jr., "Fatigue Crack Propagation in Stiffened Panels," *Damage Tolerance in Aircraft Structures*, ASTM Special Technical Publ. 486, American Society for Testing and Materials, Philadelphia, 1971, pp. 79–97.

[13]Niu, M. C. Y., *Airframe Structural Design*, Commilit Press, Hong Kong, PRC, 1988, Chap. 5.

[14] *Use of Linear Elastic Fracture Mechanics in Estimating Fatigue Crack Growth Rates and Residual Strength Component*, ESDU 80036, Engineering Sciences Data Units, London, 1991, p. 155.

[15] Galatolo, R., and Lanciotti, A., "Fatigue Crack Propagation in Residual Stress Fields of Welded Plates," *International Journal of Fatigue*, Vol. 19, No. 1, 1997, pp. 43–49.

[16] Edwards, L., Fitzpatrick, M. E., Irving, P. E., Sinclair, I., Zhang, X., and Yapp, D., "An Integrated Approach to the Determination and Consequences of Residual Stress on the Fatigue Performance of Welded Aircraft Structures," ASTM Meeting on Residual Stress Effect in Fatigue, May 2004; also *ASTM Journal of Testing and Evaluation* (submitted for publication).

[17] Serrano, G., "Variable Polarity Plasma Arc Welding of 12.5 mm Thick AA-2024 T351, AA-7150 T651 and AA-7150 W51," *Proceedings of 2nd International Conference on Recent Trends and Future Developments in Welding Technology*, Vol. 1, edited by D. Yapp, Cranfield Univ., Cranfield, England, U.K., 2003, pp. 1–12.

[18] Theos, A., and Zhang, X., "Finite Element Analysis of Fatigue Crack Growth in Plasma Welded 2024-T351 Aluminum Joints," Cranfield Univ., WELDES Project Report, CoA 20012, Cranfield, England, U.K., July 2002.

[19] Harter, J. A., *AFGROW Users Guide and Technical Manual*, U.S. Air Force Research Lab., AFRL-VA-WP-1999-3016, Wright–Patterson AFB, OH, Jan. 1999.

[20] Li, Y., "Analysis of Strength of Cracked Stiffened Panels," *Acta Mechanica Solida Sinica*, Vol. 19, Dec. 1998, pp. 90–95 (in Chinese).

[21] Swift, T., "Damage Tolerance in Pressurized Fuselages," ICAF, Vol. 1, edited by D. L. Simpson, Paper 1, Engineering Materials Advisory Services, Ltd., Cradley Heath, England, U.K., June 1987.

[22] Feddersen, C. E., "Evaluation and Prediction of the Residual Strength of Centre Cracked Tension Panels," *Damage Tolerance in Aircraft Structures*, ASTM Special Technical Publ. 486, American Society for Testing and Materials, Philadelphia, 1971, pp. 50–78.

[23] Kuo, A. S., "A Two-Dimensional Shear Spring Element," *AIAA Journal*, Vol. 22, No. 10, 1984, pp. 1460–1464.

B. Sankar
Associate Editor